Strong multiphoton absorption properties of one styrylpyridinium salt in a highly polar solvent

Tingchao He,[1] Song Yao,[1] Junmin Zhang,[2] Yiwei Li,[3] Xingrong Li,[2] Juguang Hu,[1] Rui Chen,[3,4] and Xiaodong Lin[1,5]

[1]*College of Physics and Energy, Shenzhen University, Shenzhen 518060, China*
[2]*College of Chemistry and Environmental Engineering, Shenzhen University, Shenzhen 518060, China*
[3]*Department of Electrical and Electronic Engineering, South University of Science and Technology of China, Shenzhen 518055, China*
[4]*chen.r@sustc.edu.cn*
[5]*linxd@szu.edu.cn*

Abstract: Multiphoton absorption (MPA) effects have become useful for real applications as well as conceptual predictions. However, most of organic molecules exhibit small Stokes shift and reduced MPA in the highly polar solvents, which may seriously hinder their related applications. In this work, one styrylpyridinium salt has been synthesized, which exhibits outstanding properties such as bright red fluorescence at the wavelength of 626 nm in a highly polar solvent (DMSO). Importantly, it is noted that the material also exhibits strong two- and three-photon absorption action cross-section (δ_{2PA} = 597 GM and δ_{3PA} = 18 × 10^{-80} $cm^6 \cdot s^2 \cdot photon^{-2}$, respectively), which can be excited in near-infrared (NIR) window I (650–900 nm) and NIR window II (1000–1450 nm). Meanwhile, two-photon *in vitro* bioimaging and MPA induced optical limiting behavior have been successfully demonstrated based on the chromophore.

OCIS codes: (190.4180) Multiphoton processes; (300.6410) Spectroscopy, multiphoton.

References and links

1. G. S. He, L. S. Tan, Q. Zheng, and P. N. Prasad, "Multiphoton Absorbing Materials: Molecular Designs, Characterizations, and Applications," Chem. Rev. **108**(4), 1245–1330 (2008).
2. S. Kim, T. Y. Ohulchanskyy, H. E. Pudavar, R. K. Pandey, and P. N. Prasad, "Organically Modified Silica Nanoparticles Co-encapsulating Photosensitizing Drug and Aggregation-Enhanced Two-Photon Absorbing Fluorescent Dye Aggregates for Two-Photon Photodynamic Therapy," J. Am. Chem. Soc. **129**(9), 2669–2675 (2007).
3. C. M. Lemon, E. Karnas, X. Han, O. T. Bruns, T. J. Kempa, D. Fukumura, M. G. Bawendi, R. K. Jain, D. G. Duda, and D. G. Nocera, "Micelle-Encapsulated Quantum Dot-Porphyrin Assemblies as in Vivo Two-Photon Oxygen Sensors," J. Am. Chem. Soc. **137**(31), 9832–9842 (2015).
4. Q. Zheng, H. Zhu, S. Chen, C. Tang, E. Ma, and X. Chen, "Frequency-upconverted stimulated emission by simultaneous five-photon absorption," Nat. Photonics **7**(3), 234–239 (2013).
5. H. H. Fan, L. Guo, K. F. Li, M. S. Wong, and K. W. Cheah, "Exceptionally strong multiphoton-excited blue photoluminescence and lasing from ladder-type oligo(p-phenylene)s," J. Am. Chem. Soc. **134**(17), 7297–7300 (2012).
6. G. S. He, P. P. Markowicz, T.-C. Lin, and P. N. Prasad, "Observation of stimulated emission by direct three-photon excitation," Nature **415**(6873), 767–770 (2002).
7. J. Yu, Y. Cui, H. Xu, Y. Yang, Z. Wang, B. Chen, and G. Qian, "Confinement of pyridinium hemicyanine dye within an anionic metal-organic framework for two-photon-pumped lasing," Nat. Commun. **4**, 2719 (2013).
8. T. He, Z. B. Lim, L. Ma, H. Li, D. Rajwar, Y. Ying, Z. Di, A. C. Grimsdale, and H. Sun, "Large Two-Photon Absorption of Terpyridine-Based Quadrupolar Derivatives: Towards their Applications in Optical Limiting and Biological Imaging," Chem. Asian J. **8**(3), 564–571 (2013).
9. H. A. Collins, M. Khurana, E. H. Moriyama, A. Mariampillai, E. Dahlstedt, M. Balaz, M. K. Kuimova, M. Drobizhev, V. X. D. Yang, D. Phillips, A. Rebane, B. C. Wilson, and H. L. Anderson, "Blood-vessel closure using photosensitizers engineered for two-photon excitation," Nat. Photonics **2**(7), 420–424 (2008).
10. S. Ellinger, K. R. Graham, P. Shi, R. T. Farley, T. T. Steckler, R. N. Brookins, P. Taranekar, J. Mei, L. A. Padilha, T. R. Ensley, H. Hu, S. Webster, D. J. Hagan, E. W. Van Stryland, K. S. Schanze, and J. R. Reynolds, "Donor–Acceptor–Donor-based Conjugated Oligomers for Nonlinear Optics and Near-IR Emission," Chem. Mater. **23**(17), 3805–3817 (2011).

#262215 Received 30 Mar 2016; revised 30 Apr 2016; accepted 1 May 2016; published 11 May 2016

11. B. Dong, C. Li, G. Chen, Y. Zhang, Y. Zhang, M. Deng, and Q. Wang, "Facile Synthesis of Highly Photoluminescent Ag_2Se Quantum Dots as a New Fluorescent Probe in the Second Near-Infrared Window for in Vivo Imaging," Chem. Mater. **25**(12), 2503–2509 (2013).
12. D. Ding, K. Li, W. Qin, R. Zhan, Y. Hu, J. Liu, B. Z. Tang, and B. Liu, "Conjugated Polymer Amplified Far-Red/Near-Infrared Fluorescence from Nanoparticles With Aggregation-Induced Emission Characteristics for Targeted In Vivo Imaging," Adv. Healthc. Mater. **2**(3), 500–507 (2013).
13. Y. Gao, G. Feng, T. Jiang, C. Goh, L. Ng, B. Liu, B. Li, L. Yang, J. Hua, and H. Tian, "Biocompatible Nanoparticles Based on Diketo-Pyrrolo-Pyrrole (DPP) with Aggregation-Induced Red/NIR Emission for In Vivo Two-Photon Fluorescence Imaging," Adv. Funct. Mater. **25**(19), 2857–2866 (2015).
14. Y. Tan, Q. Zhang, J. Yu, X. Zhao, Y. Tian, Y. Cui, X. Hao, Y. Yang, and G. Qian, "Solvent effect on two-photon absorption (TPA) of three novel dyes with large TPA cross-section and red emission," Dyes Pigments **97**(1), 58–64 (2013).
15. J. Zhang, R. Chen, Z. Zhu, C. Adachi, X. Zhang, and C. S. Lee, "Highly Stable Near-Infrared Fluorescent Organic Nanoparticles with a Large Stokes Shift for Noninvasive Long-Term Cellular Imaging," ACS Appl. Mater. Interfaces **7**(47), 26266–26274 (2015).
16. A. L. Kanibolotsky, F. Vilela, J. C. Forgie, S. E. T. Elmasly, P. J. Skabara, K. Zhang, B. Tieke, J. McGurk, C. R. Belton, P. N. Stavrinou, and D. D. C. Bradley, "Well-defined and monodisperse linear and star-shaped quaterfluorene-DPP molecules: the significance of conjugation and dimensionality," Adv. Mater. **23**(18), 2093–2097 (2011).
17. L. Li, J. Liu, X. Yang, Z. Peng, W. Liu, J. Xu, J. Tang, X. He, and K. Wang, "Quantum dot/methylene blue FRET mediated NIR fluorescent nanomicelles with large Stokes shift for bioimaging," Chem. Commun. (Camb.) **51**(76), 14357–14360 (2015).
18. T. He, R. Chen, Z. B. Lim, D. Rajwar, L. Ma, Y. Wang, Y. Gao, A. C. Grimsdale, and H. Sun, "Efficient energy transfer under two-photon excitation in a 3D supramolecular Zn(II)-coordinated self-assembled organic network," Adv. Opt. Mater. **2**(1), 40–47 (2014).
19. H. S. Quah, W. Chen, M. K. Schreyer, H. Yang, M. W. Wong, W. Ji, and J. J. Vittal, "Multiphoton harvesting metal-organic frameworks," Nat. Commun. **6**, 7954 (2015).
20. L. Yang, Y. Liu, X. Zhou, Y. Wu, C. Ma, W. Liu, and C. Zhang, "Asymmetric anthracene-fused BODIPY dye with large Stokes shift: Synthesis, photophysical properties and bioimaging," Dyes Pigments **126**, 232–238 (2016).
21. E. Şen, K. Meral, and S. Atılgan, "From dark to light to fluorescence resonance energy transfer (FRET): polarity-sensitive aggregation-induced emission (AIE)-active tetraphenylethene-fused BODIPY dyes with a very large pseudo-stokes shift," Chemistry **22**(2), 736–745 (2016).
22. B. He, H. Nie, L. Chen, X. Lou, R. Hu, A. Qin, Z. Zhao, and B. Z. Tang, "High fluorescence efficiencies and large stokes shifts of folded fluorophores consisting of a pair of alkenyl-tethered, π-stacked oligo-p-phenylenes," Org. Lett. **17**(24), 6174–6177 (2015).
23. H. Jintoku, M. Kao, A. D. Guerzo, Y. Yoshigashima, T. Masunaga, M. Takafuji, and H. Ihara, "Tunable Stokes shift and circularly polarized luminescence by supramolecular gel," J. Mater. Chem. C Mater. Opt. Electron. Devices **3**(23), 5970–5975 (2015).
24. A. Purc, K. Sobczyk, Y. Sakagami, A. Ando, K. Kamada, and D. T. Gryko, "Strategy towards large two-photon absorption cross-sections for diketopyrrolopyrroles," J. Mater. Chem. C Mater. Opt. Electron. Devices **3**(4), 742–749 (2015).
25. S. L. Oliveira, D. S. Corrêa, L. Misoguti, C. J. L. Constantino, R. F. Aroca, S. C. Zilio, and C. R. Mendonça, "Perylene derivatives with large two-photon-absorption cross-sections for application in optical limiting and upconversion lasing," Adv. Mater. **17**(15), 1890–1893 (2005).
26. M. Albota, D. Beljonne, J. L. Brédas, J. E. Ehrlich, J. Y. Fu, A. A. Heikal, S. E. Hess, T. Kogej, M. D. Levin, S. R. Marder, D. McCord-Maughon, J. W. Perry, H. Röckel, M. Rumi, G. Subramaniam, W. W. Webb, X.-L. Wu, and C. Xu, "Design of organic molecules with large two-photon absorption cross sections," Science **281**(5383), 1653–1656 (1998).
27. J. E. Ehrlich, X. L. Wu, I.-Y. S. Lee, Z.-Y. Hu, H. Röckel, S. R. Marder, and J. W. Perry, "Two-photon absorption and broadband optical limiting with bis-donor stilbenes," Opt. Lett. **22**(24), 1843–1845 (1997).
28. T. He, S. Sreejith, Y. Gao, A. C. Grimsdale, Y. Zhao, X. Lin, and H. Sun, "Superior optical nonlinearity of an exceptional fluorescent stilbene dye," Appl. Phys. Lett. **106**(11), 111904 (2015).
29. M. Sheik-Bahae, A. A. Said, T. H. Wei, D. J. Hagan, and E. W. Van Stryland, "Sensitive measurement of optical nonlinearities using a single beam," IEEE J. Quantum Electron. **26**(4), 760–769 (1990).
30. R. L. Sutherland, *Handbook of Nonlinear Optics*, 2nd ed. (New York, 2003).
31. L. Ma, Y. Zhang, and P. Yuan, "Nonlinear optical properties of phenoxy-phthalocyanines at 800 nm with femtosecond pulse excitation," Opt. Express **18**(17), 17666–17671 (2010).
32. G. S. He, G. C. Xu, P. N. Prasad, B. A. Reinhardt, J. C. Bhatt, and A. G. Dillard, "Two-photon absorption and optical-limiting properties of novel organic compounds," Opt. Lett. **20**(5), 435–437 (1995).
33. G. S. He, J. D. Bhawalkar, P. N. Prasad, and B. A. Reinhardt, "Three-photon-absorption-induced fluorescence and optical limiting effects in an organic compound," Opt. Lett. **20**(14), 1524–1526 (1995).
34. R. Orłowski, M. Banasiewicz, G. Clermont, F. Castet, R. Nazir, M. Blanchard-Desce, and D. T. Gryko, "Strong solvent dependence of linear and non-linear optical properties of donor-acceptor type pyrrolo[3,2-b]pyrroles," Phys. Chem. Chem. Phys. **17**(37), 23724–23731 (2015).
35. X. Shi, Z. Xu, Q. Liao, Y. Wu, Z. Gu, R. Zheng, and H. Fu, "Aggregation enhanced two-photon fluorescence of organic nanoparticles," Dyes Pigments **115**, 211–217 (2015).

#262215 Received 30 Mar 2016; revised 30 Apr 2016; accepted 1 May 2016; published 11 May 2016

36. L. Guo and M. S. Wong, "Multiphoton excited fluorescent materials for frequency upconversion emission and fluorescent probes," Adv. Mater. **26**(31), 5400–5428 (2014).
37. D. H. Friese, A. Mikhaylov, M. Krzeszewski, Y. M. Poronik, A. Rebane, K. Ruud, and D. T. Gryko, "Pyrrolo[3,2-b]pyrroles-From Unprecedented Solvatofluorochromism to Two-Photon Absorption," Chemistry **21**(50), 18364–18374 (2015).
38. M. Pawlicki, H. A. Collins, R. G. Denning, and H. L. Anderson, "Two-Photon Absorption and the Design of Two-Photon Dyes," Angew. Chem. Int. Ed. Engl. **48**(18), 3244–3266 (2009).
39. H. Myung Kim and B. Rae Cho, "Two-photon materials with large two-photon cross sections. Structure-property relationship," Chem. Commun. (Camb.) **49**(2), 153–164 (2009).
40. C. Huang, X. Peng, D. Yi, J. Qu, and H. Niu, "Dicyanostilbene-based two-photon thermo-solvatochromic fluorescence probes with large two-photon absorption cross sections: Detection of solvent polarities, viscosities, and temperature," Sensor Actuate-Chem. **182**, 521–529 (2013).
41. M. Wielgus, J. Michalska, M. Samoc, and W. Bartkowiak, "Two-photon solvatochromism III: Experimental study of the solvent effects on two-photon absorption spectrum of p-nitroaniline," Dyes Pigments **113**, 426–434 (2015).
42. A. K. Mandal, S. Sreejith, T. He, S. K. Maji, X. J. Wang, S. L. Ong, J. Joseph, H. Sun, and Y. Zhao, "Three-photon-excited luminescence from unsymmetrical cyanostilbene aggregates: morphology tuning and targeted bioimaging," ACS Nano **9**(5), 4796–4805 (2015).
43. C. Xu, W. Zipfel, J. B. Shear, R. M. Williams, and W. W. Webb, "Multiphoton fluorescence excitation: new spectral windows for biological nonlinear microscopy," Proc. Natl. Acad. Sci. U.S.A. **93**(20), 10763–10768 (1996).
44. Y. Qian and M. Luo, "Synthesis and efficient three-photon excited green fluorescence of pyridine-triphenylamine conjugated dyes," Dyes Pigments **101**, 240–246 (2014).
45. T. Jadhav, R. Maragani, R. Misra, V. Sreeramulu, D. N. Rao, and S. M. Mobin, "Design and synthesis of donor-acceptor pyrazabole derivatives for multiphoton absorption," Dalton Trans. **42**(13), 4340–4342 (2013).
46. P. V. Simpson, L. A. Watson, A. Barlow, G. Wang, M. P. Cifuentes, and M. G. Humphrey, "Record Multiphoton Absorption Cross-Sections by Dendrimer Organometalation," Angew. Chem. Int. Ed. Engl. **55**(7), 2387–2391 (2016).
47. A. Kumar, L. Li, A. Chaturvedi, J. Brzostowski, J. Chittigori, S. Pierce, L. A. Samuelson, D. Sandman, and J. Kumar, "Two-photon fluorescence properties of curcumin as a biocompatible for confocal imaging," Appl. Phys. Lett. **100**(20), 203701 (2012).

1. Introduction

Multiphoton absorption (MPA) is of great theoretical and practical interests in a range of scientific and technical fields including photodynamic therapy, frequency upconverted lasing/stimulated emission, optical limiting (OL) and bioimaging *etc* [1–9]. Moreover, different requirements are needed to satisfy diverse application scenarios. For the application of bioimaging, the major factors that limit the penetration depth of excitation light include absorption and scattering from biological tissue and water. To overcome this problem, much efforts have been made to design and synthesize MPA molecules that can emit far-red/near-infrared (FR/NIR) fluorescence and also can be excited in the "biological transparency window", that is, NIR window I (650–900 nm) and NIR window II (1000–1450 nm) [10,11]. Moreover, the light in NIR window II will have larger penetration depth than that in NIR window I. However, structurally stable dyes emitting FR/NIR fluorescence and exhibiting strong MPA in "biological transparency window" are still scarce at present. Meanwhile, due to their planar aromatic structures, FR/NIR fluorescent molecules are easy to aggregate in highly polar media which results in significantly reduced uorescence quantum yield (QY) [12–14]. Another desired feature for the application of bioimaging is a large Stokes shift of MPA molecules [15,16]. However, typical FR/NIR fluorescent molecules generally have small Stokes shift in the range of 10–20 nm. Although energy transfer between two dyes can increase the Stokes shift significantly, such kinds of systems could be difficult to synthesize [17–21]. As for the application of MPA based on OL, the compounds should display good solubility and large MPA in organic solvents.

Although there are numerous examples of conjugated organic compounds that show large MPA in organic solvents, previous literatures usually reported relatively small Stokes shift and narrow broad tunability of Stokes shift in solvent with different polarity [22–24]. Moreover, in contrast to the case of solvents with high polarity, for these compounds, lowly polar solvents usually result in much larger MPA and much higher QY, which are not beneficial for the application of bioimaging. Meanwhile, from the viewpoint of applications, combining different applications together should be extremely important. Unfortunately, most

#262215 Received 30 Mar 2016; revised 30 Apr 2016; accepted 1 May 2016; published 11 May 2016

known organic molecules are designed and developed for single purpose, which hinders the full exploitation of MPA materials. Therefore, there is an urgent need to develop MPA materials with the suitable combination of different applications [25]. Stilbene chromophores have been found to be one kind of excellent multiphoton absorbing molecules [26,27]. We also found one kind of stilbene chromorphores showed more efficient MPA in highly polar solvent than many D-π-A or quadrupolar chromophore [28]. To gain further insights into the enhancement of MPA, in this work, the stilbene uorophore was further modified in order to obtain its pyridinium salt with enhanced intramolecular charge transfer (ICT). Based on the experimental results, we find that the pyridinium salt indeed exhibit enhanced two- and three-photon absorption (2- and 3PA) behaviors in highly polar solvents, indicating that it is a useful probe for multiphoton excited fluorescence microscopy and is a promising building block as MPA-based optical limiter.

2. Methods and characterization techniques

2.1. Material synthesis

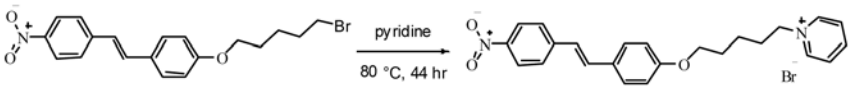

Fig. 1. The synthesis protocol of styrylpyridinium salt.

The synthesis protocol of styrylpyridinium salt ((E)-1-(6-(4-(4-nitrostyryl)phenoxy)hexyl)pyridin-1-ium bromide) was outlined in Fig. 1. (E)-4-(4-((6-bromohexyl)oxy)styryl)aniline (0.23g, 0.57 mmol) was dissolved in 25 mL of pyridine, and heated at 80 °***C*** for 44 hrs. Then pyridine was removed using rotary evaporator, and the solid residue was washed with diethylether and ethyl acetate under sonication for three times. Brown sticky solid was then dried (0.26 g, 94.5%). ^{1}H NMR (400 MHz, $CDCl_3$) δ 9.48 (d, J = 8 Hz), 8.47 (t, J = 8 Hz, 1 H), 8.19 (d, J = 8 Hz, 2 H), 8.10 (t, J = 8 Hz, 2 H), 7.58 (d, J = 8 Hz, 2 H), 7.47 (d, J = 8 Hz, 2 H), 7.21 (d, J = 16 Hz, 2 H), 7.00 (d, J = 16 Hz, 2 H), 6.89 (d, J = 8 Hz, 2 H), 5.06, (t, J = 8 Hz, 2 H), 3.96 (t, J = 6.4 Hz, 2 H), 2.09 (m, 2H), 1.74 (m, 2H) 1.54-1.46 (br, 4H). ^{13}C NMR (100 MHz, $CDCl_3$) δ 159.72, 146.55, 145.25, 145.18, 144.43, 133.03, 129.02, 128.59, 128.52, 126.64, 124.28, 124.18, 115.02, 67.84, 49.31, 32.04, 28.96, 25.83, 25.74. HRMS (ESI) *m/z*: calcd for $C_{24}H_{25}N_2O_3^+$ $[M - Br]^+$: 389.1865, found: 389.1863.

2.2. Photophysical methods

The measurements of linear absorption, fluorescence and QY. The solutions were filled into quartz cuvettes with a 1 cm path length. UV-Vis absorption and fluorescence spectra of the samples were measured by using a Lambda 950 UV/Vis spectrometer (PerkinElmer, Inc.) and a Zolix fluorescence spectrophotometer (SENS-9000), respectively. Due to the very low QY of molecule in toluene solution, its fluorescence was excited by a focused beam from a Xenon lamp and was then collected by Ocean Optics HR4000 spectrometer. The absolute QYs of targeted compound in different solvents were determined by using an integrating sphere equipped Zolix fluorescence spectrophotometer.

Lifetime measurements. Lifetime measurements were carried out at room temperature by the time-correlated single photon counting (TCSPC) technique with a resolution of 10 ps (PicoQuant PicoHarp 300). The second harmonic of a titanium–sapphire laser (Chameleon, Coherent Inc.) at 360 nm (100 fs, 80 MHz) was used as the excitation source.

The determination of MPA cross-sections. The 2- and 3PA cross-sections of samples were measured by Z-scan technique [28]. In Z-scan measurements, a femtosecond amplified-pulsed laser system (Spectra-Physics, Spitfire Pro) was used as the laser source. The output wavelengths ranging from 250 nm to 2.6 μm can be continuously tuned through an optical parameter amplifier (regen) combined with an optical parametric oscillator (TOPAS). The pulse-width and repetition rate are 100 fs and 1 KHz, respectively. The compound was firstly dissolved in the organic solvents to obtain solutions of 1 mM concentration, and then the

#262215 Received 30 Mar 2016; revised 30 Apr 2016; accepted 1 May 2016; published 11 May 2016

solutions were filled into quartz cuvettes with a thickness of 1 mm, which were traversed in the focusing geometry enabled by an achromat lens of 200 mm focal length. Typical energies in the range of 70–400 GW/cm^2 were used for all the measurements. The experimental errors were smaller than 10% and 15% in the measurements of 2- and 3PA cross-sections, respectively, arising from the uncertainties due to fluctuation of pulse energy or/and light scattering effect. Theoretically, the 2PA-induced decrease of transmissivity in the open aperture Z-scan measurements can be expressed as

$$T_{OA}(2PA) = \frac{1}{1+\beta L_{\text{eff}}^{2PA}(I_{00}/(1+(z/z_0)^2))} \tag{1}$$

where I_{00} is the incident intensity, z is the position of sample, z_0 is the diffraction length of the beam, L_{eff}^{2PA} ($L_{\text{eff}}^{2PA}=(1-e^{-\alpha_0 L})/\alpha_0 L$, α_0 is the linear absorption coefficient) is the effective thickness of the sample, and β (in unit of cm/GW) is the 2PA coefficient of the sample [29–31]. Furthermore, the 2PA cross-section (δ_{2PA}, in unit of cm^4 photon^{-1} s^{-1}) is determined by

$$\delta_{2PA} = \frac{\beta \cdot h\nu}{N_A d \times 10^{-3}} \tag{2}$$

where d is the concentration of the 2PA compound in the solution (in unit of M/L) and N_A is the Avogadro constant [32]. In the case of 3PA, the open aperture Z-scan data can be expressed as

$$T_{OA}(3PA) = \frac{1}{[1+2\gamma L_{\text{eff}}^{3PA}(I_{00}/(1+(z/z_0)^2))^2]^{1/2}} \tag{3}$$

where γ is the 3PA coefficient of the sample (in unit of cm^3/GW^2), $L_{\text{eff}}^{3PA}=(1-e^{-2\alpha_0 L})/2\alpha_0 L$ is the effective thickness of the sample [29–31]. Meanwhile, the 3PA cross-section (in unit of cm^6 s^2 photon^{-2}) can be determined according to

$$\delta_{3PA} = \frac{\gamma \cdot (h\nu)^2}{N_A d \times 10^{-3}} \tag{4}$$

where δ_{3PA} represents the molecular 3PA cross-section [33].

Two- and three-photon excited fluorescence Spectra. Multiphoton excited fluorescence spectra were measured by using the same excitation source used in Z-scan measurements. To avoid the reabsorption effect due to high concentration of the molecule, the solutions were freshly prepared at a concentration of 1 × 10^{-4} M. The laser beam was focused as close as possible to the wall of the quartz cell and the fluorescence signals were collected in back-scattering geometry, so that only the emission from the edge of the solution was collected by the Ocean Optics HR4000 spectrometer.

Two-photon bioimaging. The HeLa cancer cells were firstly cultured in confocal microscope dishes at 5 × 10^5/mL in complete Dulbecco's modified Eagle's medium (DMEM, Gibco, America) for 24 h at 37 °C. After that, the cultured cells were washed with phosphate buffered saline (PBS) three times and then incubated for 4 h with the medium containing the chromophore. Finally, the cells were washed twice with PBS. Two-photon cell imaging was acquired using a confocal laser scanning microscope (CLSM) (Zeiss LSM 410) with imaging software (Fluoview FV500), under the excitation of fs 800 nm.

3. Results and discussion

3.1. Linear photophysical properties of the styrylpyridinium salt

The styrylpyridinium salt was slightly soluble in lowly polar solvents, such as toluene, while it could be well dissolved in organic solvents with mediate to high polarity, such as

#262215 Received 30 Mar 2016; revised 30 Apr 2016; accepted 1 May 2016; published 11 May 2016

chloroform ($CHCl_3$), tetrahydrofuran (THF), acetone, dimethylformamide (DMF) and dimethylsulphoxide (DMSO). The one-photon absorption (1PA) and emission spectra of the chromophore in different solvents are shown in Fig. 2. It could be known that the shapes of the absorption spectra of the compound were very similar and displayed intense absorption bands located at 380-420 nm. Meanwhile, it was found that the 1PA spectrum was relatively insensitive to the changes in the polarity of the environment, with only a small shift of 25 nm (or 0.22 eV) in different solvents. By contrast, the maximum emission wavelength was red-shifted by 116 nm (or 0.45 eV) from 510 nm in toluene to 626 nm in DMSO. The large bathochromic shift of the emission band with increasing solvent polarity indicated better stabilization of the excited state in highly polar solvents. Such a behavior was the characteristic of enlarged dipole moment and charge transfer character in the excited state [34,35]. Notably, the chromophore in DMSO exhibited a very large Stokes shift of 237 nm, which represented one of the largest values among fluorescent materials [14–16]. It indicated that significant charge redistribution occurred upon excitation and the emission originated from a strongly dipolar emissive state. Furthermore, the fluorescence spectrum of the chromophore in DMSO extended to 850 nm, which meant that molecular fluorescence was within the NIR window I (as highlighted in shadow color in Fig. 2). Upon increasing the solvent polarity, the absolute uorescence QYs increased from toluene (<0.1%) to DMSO (30%) due to reduced nonradiative recombination. This behavior was completely different to previous reports in which the QYs decreased with the increase of solvents' polarity [12,13].

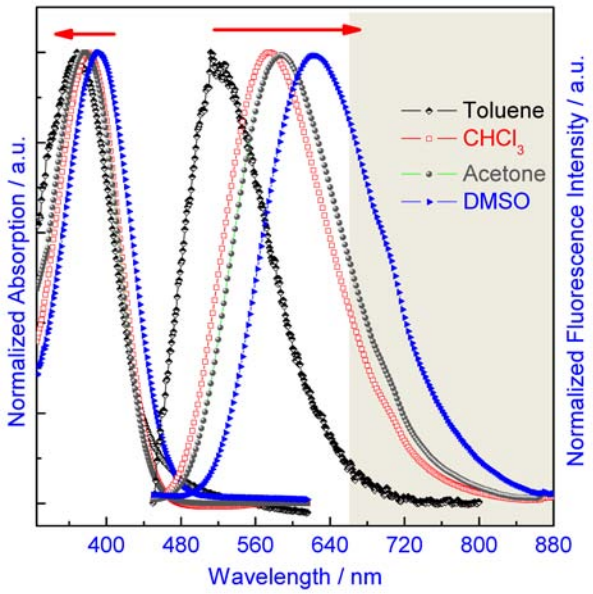

Fig. 2. Linear absorption and fluorescence emission spectra of the styrylpyridinium salt in different organic solvents. The “biological transparency window” is indicated in shadow color.

We also measured the uorescence lifetime of the dye in different solvents. The emission decay curves of the studied dye in differently polar solvents under the excitation of 360 nm is shown in Fig. 3. The lifetime of toluene solution could not be determined due to its very weak fluorescence. The values of decay time for $CHCl_3$ and acetone solutions can be well fitted with a single-exponential function while a double-exponential function was used to well fit the decay curve for the DMSO, giving average uorescence lifetime values of 1.4, 1.7 and 1.8 ns for $CHCl_3$, acetone and DMSO solutions, respectively. Obviously, the obtained results indicated that the calculated lifetime values correlated with the uorescence QYs for the chromophore in the different solvents.

#262215 Received 30 Mar 2016; revised 30 Apr 2016; accepted 1 May 2016; published 11 May 2016

In order to know the ICT process more clearly, molecular orbitals of the highest occupied molecular orbital (HOMO) and lowest unoccupied molecular orbital (LUMO) for the ground state of the studied dye in the gas phase have been visualized in Fig. 4. The color dots represented electron cloud. The shapes of the two frontier orbitals for the chromophore confirmed that the HOMO was concentrated at pyridine group while the LUMO electron density was located mainly on the styrene center and nitro-group of the chromophore, a typical feature of the ICT state. The computed results confirmed that different density polarizations took place for the studied compound, indeed resulting in an excited state that was more polar than the ground state and hence was better stabilized by polar solvents [34,35].

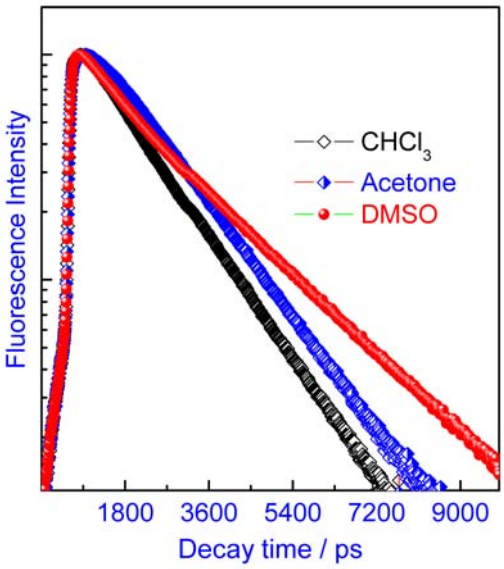

Fig. 3. Fluorescence decay profiles of the styrylpyridinium salt in different organic solvents.

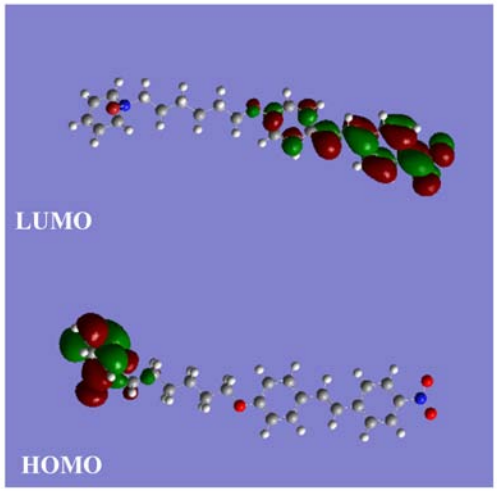

Fig. 4. Optimized frontier HOMO/LUMO of stilbene chromophore calculated with DFT at the B3LYP/6-31G(d) level by applying the Gaussian 09 program. The color dots represent electron cloud.

#262215 Received 30 Mar 2016; revised 30 Apr 2016; accepted 1 May 2016; published 11 May 2016

3.2. Solvent dependent 2- and 3PA properties

Subsequently, 2PA properties of these molecules were investigated. Upon excitation with femtosecond pulses at 800 nm, the chromophore emitted orange to red fluorescence from $CHCl_3$ to DMSO solutions. Since linear absorption beyond 600 nm were absent for studied chromophore, thus observed fluorescence was plausibly attributed to 2PA. Such a mechanism was further confirmed through the measurements of power dependent fluorescence intensity. Figure 5(a) depicts the logarithmic plots of the two-photon excited uorescence integral versus pumped power with a slope of around 2, suggesting a 2PA mechanism [36]. Subsequently, by using the method of Z-scan measurements, the 2PA spectra of the chromophore was obtained (Fig. 5(b)). The δ_{2PA} of the chromophore in toluene could not be determined with Z-scan technique due to negligible solubility. Furthermore, MPA of the chromophore in toluene also could not be measured using fluorescence comparison method, due to its weak multiphoton excited fluorescence. The chromophore exhibited effcient 2PA behavior in a relatively broad range of wavelengths between 740 and 840 nm (Fig. 5(b)), well corresponding to the double energy of linear absorption peak. The maximum δ_{2PA} which centered at around 800 nm was 563 GM in $CHCl_3$, 974 GM in acetone and 1991 GM in DMSO, respectively. These values were even larger than those of pyrrolo[3,2-b]pyrroles in lowly polar solvents [37]. It was particularly interesting because of the importance in practical applications. Two-photon excitation fluorescence microscopy usually makes use of a Ti:sapphire oscillator, which has a central wavelength of around 800 nm. Meanwhile, the enhancement of δ_{2PA} with the incremental solvent polarity was observed, due to the increased charge separation assisted by highly polar solvent and the resulted change in electronic structure that provided the main perturbation on δ_{2PA}. Most of the reports on MPA fluorescent probes focused only on either the enhancement of the fluorescence QY (Φ) or the MPA cross-section [38]. However, one must maximize the product of Φ and MPA cross-section to guarantee a sensitive response in bioimaging [39]. The 2PA action cross-section of the styrylpyridinium salt in $CHCl_3$, acetone and DMSO was calculated to be 46, 166 and 597 GM, respectively. The value in DMSO was among the largest 2PA action cross-sections of organic molecules in highly polar solvents [40,41].

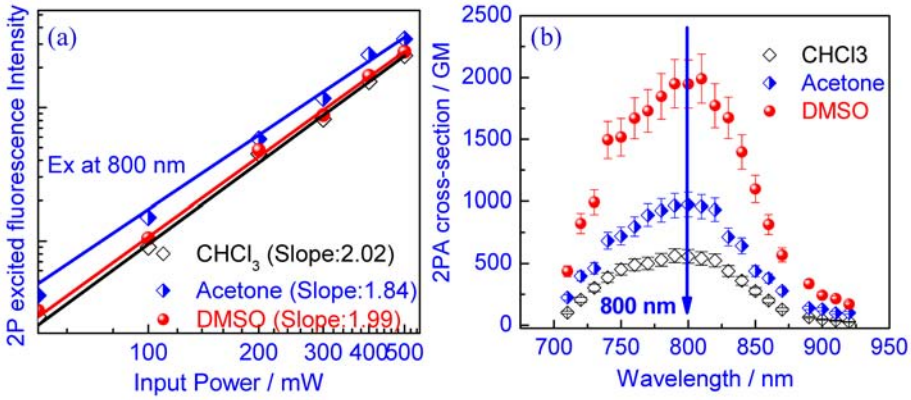

Fig. 5. (a) Quadratic dependence of 2PA induced emission intensity on the excitation intensity in different organic solvents. (b) 2PA spectra of styrylpyridinium salt in different solvents. The arrow indicates the wavelength of 800 nm, which is the central wavelength of a Ti:sapphire oscillator. Error bars indicate experimental uncertainty of ± 10%.

In addition to 2PA, 3PA is an even more intriguing and attractive photophysical phenomenon, due to the maximum penetration depth, the minimum confined volume and scattering, and the highest damage threshold, *etc* [42]. Upon irradiation with 1050 nm pulses, the chromophore exhibited nearly identical emission spectrum to those observed under one- and two-photon excitation conditions. To verify the 3PA mechanism, the integrated uorescence intensities were plotted vs laser beam intensity, as shown in Fig. 6(a). The slopes

#262215 Received 30 Mar 2016; revised 30 Apr 2016; accepted 1 May 2016; published 11 May 2016

of the log–log dependence of the uorescence intensity upon irradiation intensity in different solvents were found to be about 3, the value expected for a 3PA mechanism [43]. Next, in order to take advantage of the 3PA properties, we assessed the overall 3PA spectra around 1000 to 1500 nm using the Z-scan technique (Fig. 6(b)). For all solutions, the 3PA maximum values were observed at around three times the wavelengths of linear absorption peak of the chromophore. The maximum values of molecular 3PA cross-section (δ_{3PA}) for the chromophore in $CHCl_3$, toluene and DMSO were 17, 32 and 59 × 10^{-80} $cm^6 \cdot s^2 \cdot photon^{-2}$, corresponding to 3PA action cross-section of 1.4, 5.4 and 18 × 10^{-80} $cm^6 \cdot s^2 \cdot photon^{-2}$, respectively. Those values were significantly higher compared to many organic molecules [43–45]. Again, the high solvent polarity was beneficial for the enhancement of 3PA. Compared to those of our previous stilbene chromorphore, the MPA properties of the styrylpyridinium salt can be greatly improved due to its larger conjugation length [28]. To investigate whether or not there was aggregation of ground and/or excited states at the concentrations used to measure MPA, concentration-dependent (in the range between 1 × 10^{-6} to 1 × 10^{-3} M) linear absorption measurements were performed. It was found that the observed absorbance was linearly dependent on the concentration of the measured samples, thus indicating that no aggregation of the chromophore took place. Therefore, there was negligible influence of aggregation on the photophysical properties and the measured MPA (see Table 1).

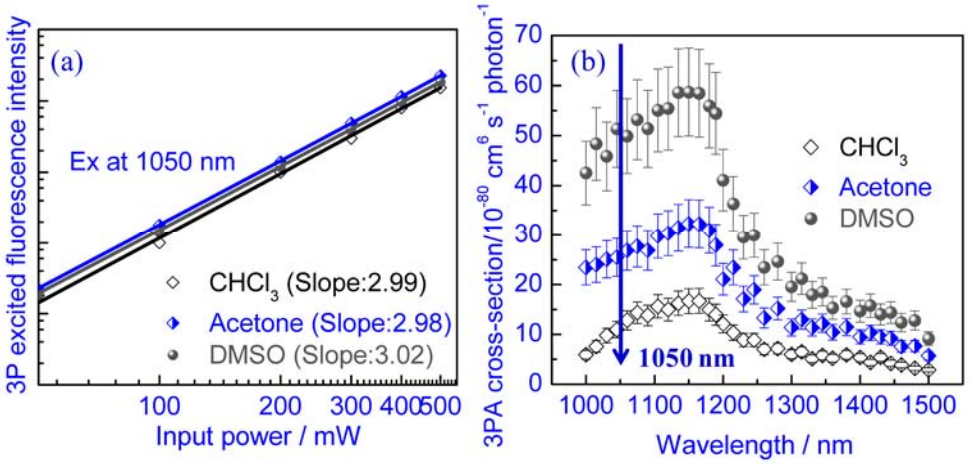

Fig. 6. (a) Cubic dependence of 3PA induced emission intensity on the excitation intensity in different organic solvents. (b) 3PA spectra of styrylpyridinium salt in different solvents. The arrow indicates the wavelength of 1050 nm, which is compatible with the 1050 nm fiber laser source. Error bars indicate experimental uncertainty of ± 15%.

Table 1. Experimental Linear and MPA Photophysical Properties of the Styrylpyridinium Salt in Different Solvents

Solvent[a]	λ_{abs}[b] (nm)	λ_{ems}[c] (nm)	τ[d] (ns)	Φ[e] (%)	δ_{2PA}[f] (GM)	$\Phi\delta_{2PA}$[g] (GM)	δ_{3PA}[h]/10^{-80} $cm^6 \cdot s^2 \cdot photon^{-2}$	$\Phi\delta_{3PA}$[i]/10^{-80} $cm^6 \cdot s^2 \cdot photon^{-2}$
Toluene	364	510	-	<0.1	—-	—-	—-	—-
$CHCl_3$	378	578	1.4	8.1	563	46	17	1.4
Acetone	375	587	1.7	17	974	166	32	5.4
DMSO	389	626	1.8	30	1991	597	59	18

[a]Concentration was estimated as 1 × 10^{-5} M and 1 × 10^{-4} M for 1PA, 2PA- and 3PA-related measurements, respectively; [b]1PA maximum; [c]one-photon excited uorescence emission maximum; [d]Average fuorescence lifetime under the excitation of 360 nm; [e]Absolute QY value measured by using an integrating sphere; [f]The maximum 2PA cross-section value; [g]The maximum 2PA action cross-section value; [h]The maximum 3PA cross-section value; [i]The maximum 3PA action cross-section value.

#262215 Received 30 Mar 2016; revised 30 Apr 2016; accepted 1 May 2016; published 11 May 2016

For bioimaging application, molecules with large MPA cross-section value per molecular weight (MW) are needed. The maximum values of δ_{2PA}/MW and δ_{3PA}/MW in DMSO were calculated to be 5 and 0.15, respectively. The values were in the same order of magnitude compared to the values of recently reported ruthenium alkynyl-containing dendrimers, which exhibited record MPA cross-sections [46]. Therefore, our chromophore was potentially useful for multiphoton bioimaging. It was noteworthy that in DMSO the molecular 3PA cross-sections or action cross-sections at 1050 nm for the chromophore were still very large, indicating that the chromophore was compatible with the 1050 nm fiber laser source and was promising in the application of 3PA bioimaging. Additionally, the chromophore displayed very good solubility (up to 10 mg/ml) in DMSO, it allowed us to investigate MPA based bioimaging and OL properties.

3.3. Two-photon cell imaging

It has been well known that DMSO is biocompatible and is nearly nontoxic to live cells. Therefore, the large MPA action cross-section of the chromophore in DMSO made it an attractive candidate as a two-photon imaging agent [47]. The cytotoxicity and photostability of the chromophore were also characterized and were suitable for bioimaging application (data not shown here). From the abovementioned experimental results, it was known that that the chromophore possessed strong 2- and 3PA action cross-section at 800 and 1050 nm. Nonetheless, three-photon excited fluorescence was observable at relatively high excitation power. Therefore, two-photon cell imaging experiment was carried out instead of three-photon bioimaging to demonstrate the application of multiphoton bioimaging. As seen in Fig. 7(b), two-photon fluorescence imaging of the labeled HeLa cells (λ_{ex} = 800 nm) featured bright uorescence from the chromophore presented in the cell. A comparison of the imaging in Figs. 7(a), (b) and (c) indicated that stilbene chromophore probe could penetrate the cell membrane and could be used for bioimaging. These results highlighted the potential application of styrylpyridinium salt for multiphoton uorescence microscopy.

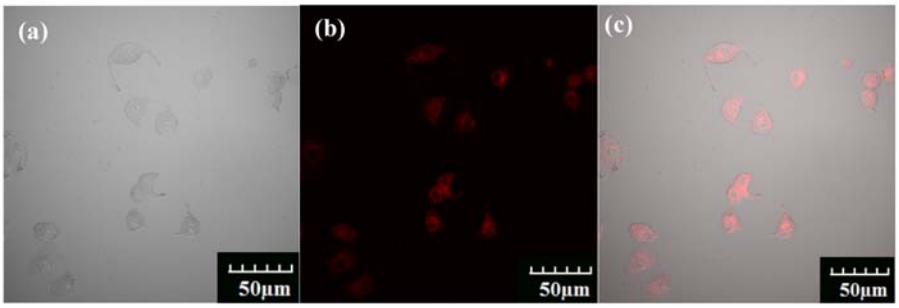

Fig. 7. (a) Bright-field imaging of HeLa cells. (b) Two-photon imaging of HeLa cells incubated with 100 μM chromophore (emission wavelength collected from 650 to 850 nm). (c) The overlay of (a) and (b). Scale bars represent 50 μm.

3.4. 2- and 3PA based OL

Due to the large MPA for the styrylpyridinium salt and good solubility in DMSO, the OL behaviors of the chromophore were investigated. Two excitation wavelengths at 800 and 1150 nm were chosen in view of 2- and 3PA mechanism at these wavelengths. In the measurements, the laser beam was focused by an f = 10 cm lens into the center of a 1 cm quartz cell filled with DMSO solution of the chromophore (0.01 M). The measured output/input relationships for the chromophore are shown in Fig. 8. It was found that at the wavelength 800 nm (corresponding to 2PA) the output/input characteristic curve started to deviate from linear transmission at optical intensity level of around 3.71 GW/cm^2. More specifically, when the input energy increased from 0.02 to 100 GW/cm^2 (5000 fold increase), the transmitted energy only changed from 0.02 to 8.67 GW/cm^2 (434 fold increase). This was

#262215 Received 30 Mar 2016; revised 30 Apr 2016; accepted 1 May 2016; published 11 May 2016

a typical OL behavior based on the 2PA. Similar behavior was also seen in the case of 3PA (at the wavelength of 1150 nm). When the input energy increased by 5000 times, the transmitted energy only exhibited 2375 fold increase. From the experimental results we found that 2- and 3PA offered excellent OL performance due to its square and cubic dependence on the incident intensity, implying that besides OL, optical stabilization may also be achieved using MPA materials.

Theoretically, the 2PA-induced decrease of transmissivity can be expressed as

$$T(I_{00}) = I(L)/I_{00} = [Ln(1+LI_{00}\beta)]/LI_{00}\beta \quad (5)$$

where I_{00} is the incident intensity, L is the thickness of the solution sample, and β is the 2PA coefficient of the solution [32]. In the case of 3PA, the transmissivity can be expressed as

$$T(I_{00}) = I(L)/I_{00} = 1/[1+2LI_{00}^2\gamma)]^{1/2} \quad (6)$$

where γ is the 3PA coefficient of the solution (in unit of cm^3/GW^2) [33]. In Fig. 8, the solid lines represent the theoretical curves given by Eqs. (5) and (6) using best fitting parameters of β = 0.48 cm/GW and γ = 1.18 × 10^{-4} cm^3/GW^2, respectively. It was found that there was fairly good agreement between results obtained the Z-scan and OL measurements.

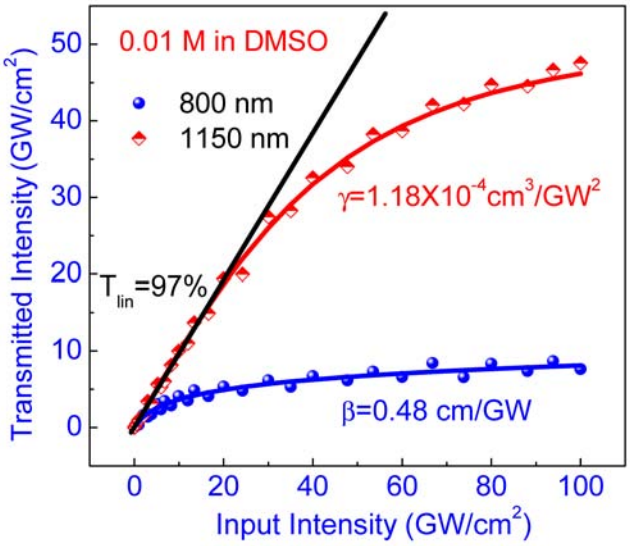

Fig. 8. Output optical intensity versus the pump intensity by two-photon excitation at 800 nm and three-photon excitation at 1150 nm, L = 1 cm, d = 0.01 M, giving a 2PA coefficient β = 0.48 cm/GW and a 3PA coefficient of γ = 1.18 × 10^{-4} cm^3/GW^2, respectively. The solid lines are fitting lines using Eqs. (5) and (6).

4. Conclusion

One pyridinium salt has been prepared, and its linear and nonlinear optical properties have been investigated. It has been found that solvent polarity has little effect on the UV–vis absorption spectra of the chromophore, while its emission spectra show systematic bathochromic shift with an increase in solvent polarity. Its emission peaks spread over a wide range of wavelengths (510–626 nm). This effect is accompanied by a giant Stokes shift (237 nm) in a highly polar solvent (DMSO) due to ICT. More importantly, the chromophore shows a high QY and efficient MPA in DMSO. In this solution, the maximum 2PA cross-section of the chromophore is 1991 GM in the NIR window I while in NIR window II the maximum 3PA cross-section with a value of 59 × 10^{-80} $cm^6 \cdot s^2 \cdot photon^{-2}$ has been obtained. The effective

#262215 Received 30 Mar 2016; revised 30 Apr 2016; accepted 1 May 2016; published 11 May 2016

MPA cross-sections in DMSO combined with a high fluorescence QY and a large Stokes shift make the compound an excellent candidate for various nonlinear absorption applications.

Acknowledgments

We thank the Natural Science Foundation of China (NSFC) Grant nos. 11404219, 11404161, and 11574130; Natural Science Foundation of Guangdong Province Grant no. 2014A030313552; Youth Innovation Talent Project (Nature Science) of the Universities of Guangdong Province Grant no. 2014KQNCX127; Shenzhen Basic Research Project of Science and Technology under Grants JCYJ20150324141711613, JCYJ20150324141711581, and JCYJ20150630162649956. We also thank Yang Gao for helpful discussions about the sample synthesis.

#262215 Received 30 Mar 2016; revised 30 Apr 2016; accepted 1 May 2016; published 11 May 2016